

# Energy Savings Using Centramatic Wheel Balancers

Purna Musunuru  
*ESI North America*

## 1. Introduction

With the ever-increasing demand for reduction of greenhouse gas emissions, the current need for fuel efficient transport is more than ever. This is especially true in case of light-duty vehicles (cars, small trucks, vans, SUVs, motorcycles), commercial and freight trucks both of which account for about 78% of the total energy use in the transportation sector [1]. Researchers and companies are continuously looking for ways to improve fuel efficiency. Tire imbalance is one such area where there is loss of energy when a tire is not properly balanced. This study focuses on the effect of using *Centramatic* wheel balancers on the overall energy consumption, specifically in class 8 trucks where tires are rarely in balance.

## 2. Modeling Methodology

A physical object-oriented modeling approach was followed for this project. Object-oriented (or network based) modeling is the natural way to describe any kind of physical behavior in simulation models. This modeling concept is shown in figure 1. Physical network models are formed of elements which are interconnected with each other by connections, also called as nodes. The physical relationships are then formulated in terms of potential and flow quantities. The potential quantities reside inside the connection and are identical for all the element connectors connected to it. Examples of such potential quantities are displacements, spends and accelerations in mechanics, pressures in fluids, voltages in electronics, temperatures in thermal models.

The flow quantities are the quantities for which certain balance equations must be fulfilled. For example, the forces or torques (depending on linear or rotational mechanics) at the connections in mechanics models must balance to zero.

Elements define the relationships between the potential quantities at their connectors and their internal flow quantities. For example, a translational mechanical spring relates internal force  $F$  and the displacement difference  $dx$  between its connectors via the stiffness parameter  $k$  by an equation  $F = k * dx$ .

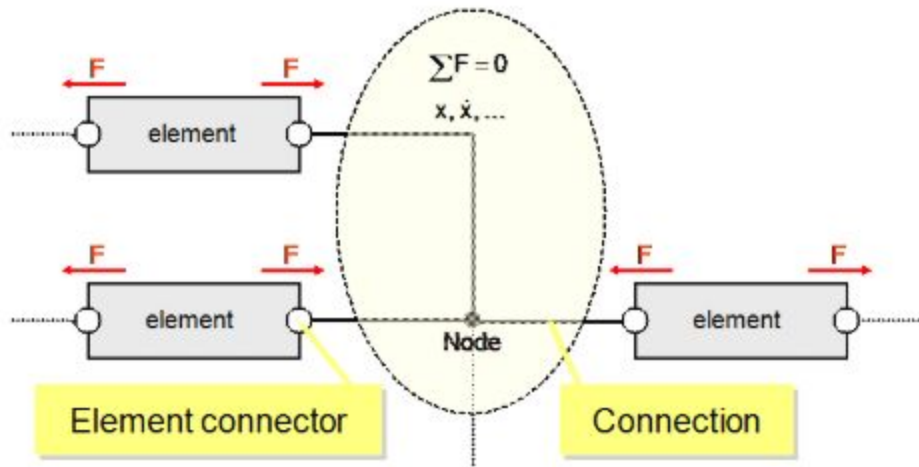


Figure 1: Modeling Concept

The models described in the following sections follow a similar methodology (elements and connections).

## 2.1 Drive and Trailer Axle Setup

This section discusses the quarter-truck setup of the tandem drive axle. Since the configuration for the drive and trailer axles is similar, the same setup is extended to the trailer axle. Figure 2 below gives an overview of the full setup and figures 3 and 4 show zoomed versions of some key elements within the setup. The elements in figure 3 are discussed from here on.

The *posDrive* element models a rigid massless link with zero degrees of freedom. This is used to fix the wheel center position as reference.

The *dofLongDrive* element is a prismatic joint representing one translational degree of freedom along a selectable axis (the longitudinal direction in this case). This prismatic joint generates two potential state variables i.e. the relative displacement and relative velocity along the longitudinal direction. Additionally, this element also gives the flexibility to model the friction and also specify actuation (either a force or a displacement or a velocity) through the linear mechanical connectors along the direction of choice.

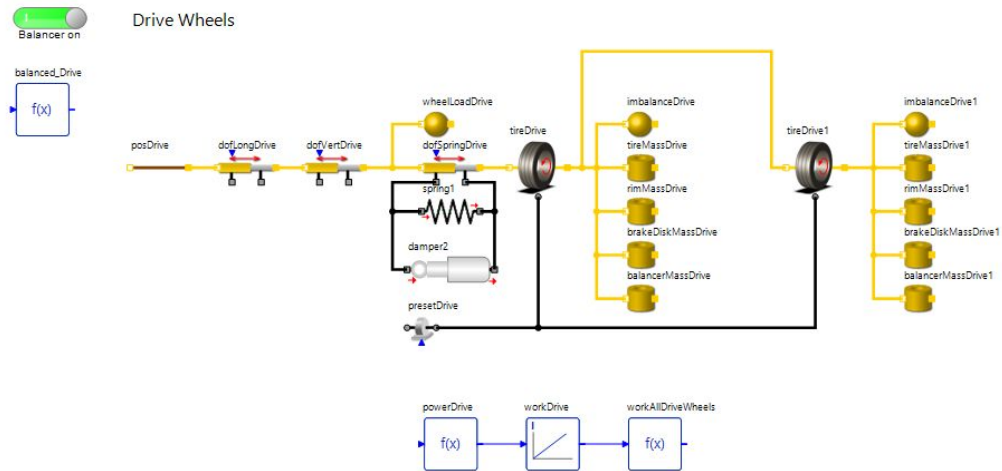


Figure 2: Drive axle full setup

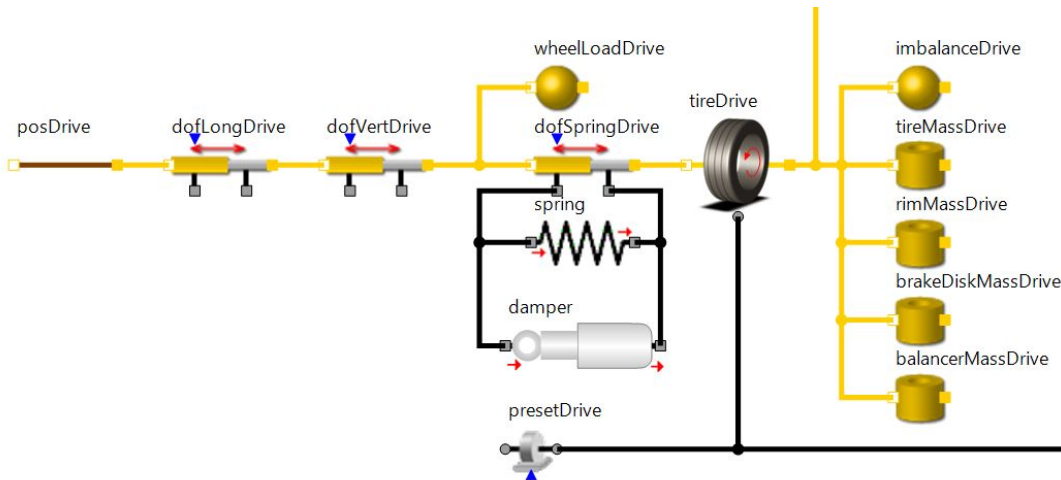


Figure 3: Drive axle – tire & wheel assembly, shock absorber setup

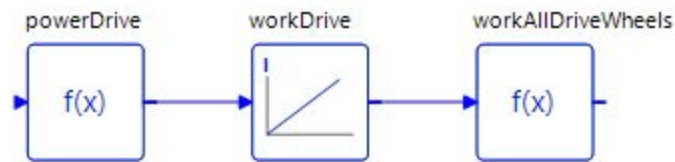


Figure 4: Drive axle – work done computation

The *dofVertDrive* element represents the same physical behavior as the *dofLongDrive*. The degree of freedom in this case is set to the vertical direction.

The *wheelLoadDrive* element is a rigid body with 6 DOF, accounting for the quarter of the total load on the tandem drive axle. Considering a truck with a GVW of 80,000 lbs, the distribution of loads on the steer, drive and trailer axles are 12,000, 34,000 and 34,000 lbs respectively. Since we are only considering a quarter of drive axle in this set-up, the mass of the *wheelLoadDrive* element is set to 8,500 lbs (34,000/4).

The flexibility due to the shock absorber in the vertical direction is then defined through the *dofSpringDrive* element. As seen, the mechanical connectors are actuated through *spring* and *damper* elements.

### 2.1.1 Spring Element

The *spring* element represents a translational stiffness describing the elastic behavior.

The internal force of the spring is computed from the following expression

$$\text{Internal force } F_i = k * dx$$

Where  $k$  is the stiffness of the spring,  $dx$  is the displacement difference which is the difference between the current displacements of the connections.

$$\text{Displacement difference } dx = ctr1.x - ctr2.x$$

To parameterize the stiffness of the spring, a full load compression of 4 inches is assumed (which is typical for shock absorbers for the 18-wheeler heavy duty trucks).

In addition to the internal force and displacement difference, the velocity difference and the change of potential energy are also computed within the spring element based on the following relations

$$\text{Velocity difference } dv = ctr1.v - ctr2.v$$

$$\text{Change of potential energy } P_p = F_i * dv$$

### 2.1.2 Damper Element

The *damper* element models the non-linear behavior described through a characteristic curve of damping coefficient. Similar to the spring element, the displacement and velocity difference are computed based on the potential variables from the connectors

$$\text{Displacement difference } dx = ctr1.x - ctr2.x$$

$$\text{Velocity difference } dv = ctr1.v - ctr2.v$$

The inner damping force is then computed based on the following relation

$$\text{Damping force } F_i = dv * bCurve(dv)$$

Where  $bCurve(dv)$  is the non-linear damping curve i.e. damping constant defined as a function of velocity difference. This non-linear damping curve is parameterized based on the literature [2] as shown in figure 5.

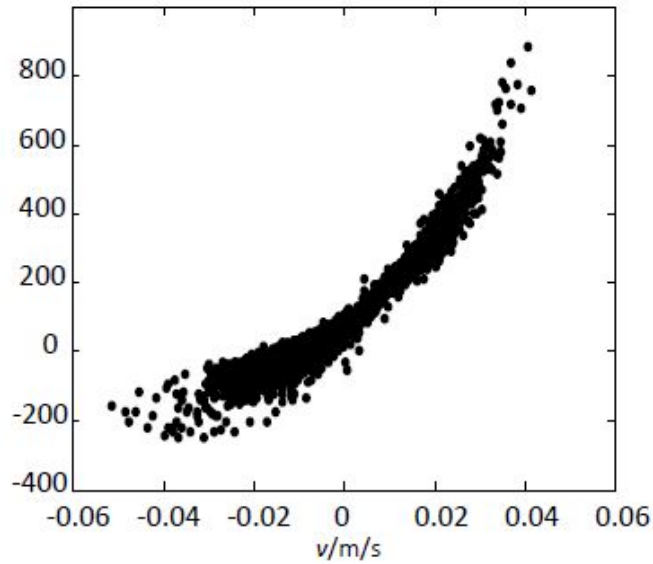


Figure 5: Non-linear shock absorber damping curve

For region outside of  $\pm 0.06 \text{ m/s}$ , a linear extrapolation technique is implemented. Finally, the power loss in the damper element is computed as follows

$$\text{Power loss } P_l = F_i * dv$$

### 2.1.3 Tire Model

The *tireDrive* element models a pneumatic tire which is regarded as a spring and damper element between hub and road surface. This element does not consider any inertia and hence rigid bodies need to be connected to model the rim, tire, brake disk inertias.

Figure 6 illustrates different coordinate systems of the tire. This description is consistent with the Tyre Data Exchange (TYDEX) format [3].

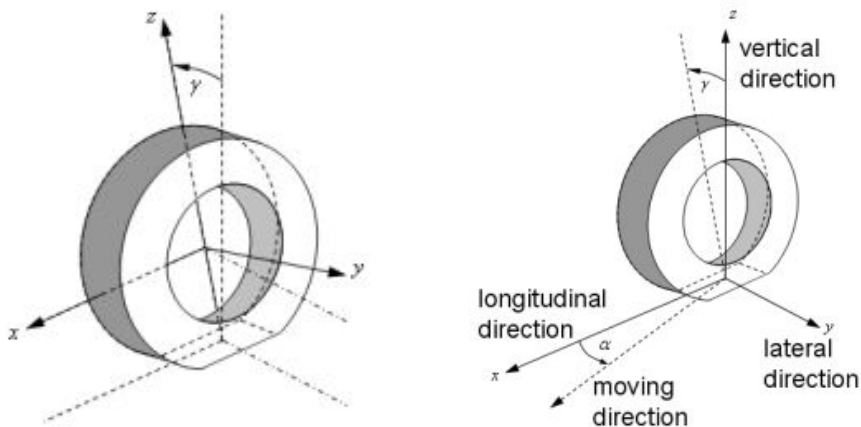


Figure 6: Tire co-ordinate systems in TYDEX format

The X-axis of the TYDEX center axis coordinate system is in the central plane of the wheel and is parallel to the ground. The driving or braking torque acts around the axis of wheel rotation, i.e. the Y-axis of the TYDEX center axis coordinate system as seen in figure 6.

Depending on the nominal wheel load, a contact area (tread shuffle) emerges between road and tire. Due to the pressure distribution along the tread shuffle, a friction force is then generated if there is a difference velocity between road and tire. This force distribution is summed up as vectors of tire forces and tire torques acting at the contact point between road and tire (wheel intersection point). This contact point is the origin of the TYDEX wheel axis coordinate system as seen in figure 6. The X-axis of the TYDEX wheel axis coordinate system is parallel to the X-axis of the TYDEX center axis coordinate system. The Y-axis is given by the projection of the axis of wheel rotation onto the ground. The Z-axis is normal to the ground and points upwards.

The side slip angle  $\alpha$  is defined as the angle between moving and longitudinal direction. The camber angle  $\gamma$  is the angle between the Z-axes of the TYDEX wheel and center axis coordinate systems.

The resulting tire forces and torques then depend on the slip values in longitudinal and lateral direction. The slip value  $\lambda$  increases with increasing driving torque and there is a non-linear relationship between the friction behavior and the tire force as seen in figure 7. For small slip values, i.e. when the tire sticks to the road, the force increases linearly. If the slip value exceeds a certain threshold, the tire then starts to slip. The final force of the sliding friction  $F_{Slip}$  is less than the maximum force  $F_{Max}$  of the static friction as the slip value approaches 1.

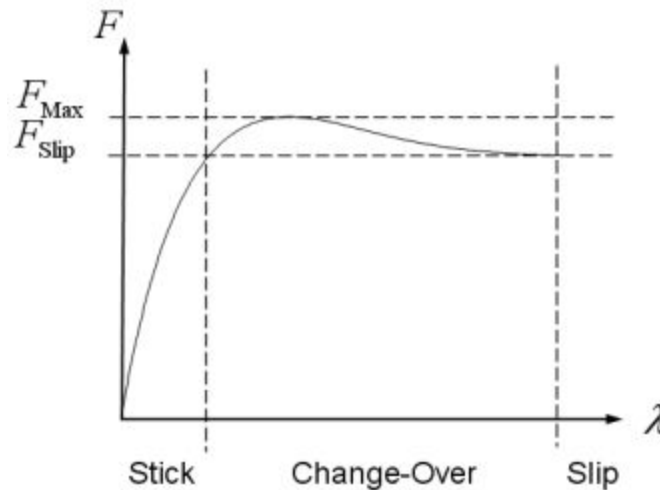


Figure 7: Tire slip characteristic curve

Based on this, the tire forces and torques are then calculated using the semi-empirical *Pacejka Tire Model* [4].

It uses only one formula with different sets of parameters for the each computation, i.e. the longitudinal force, the lateral force and the self-aligning torque. The basic equation of this magic formula is

$$f_{Magic}(x) = D \sin \sin (C \arctan \arctan (B(1-E)(x+S_H) + E \arctan \arctan (B(x+S_H))) ) + S_V$$

with stiffness factor  $B$ , shape factor  $C$ , peak value  $D$ , curvature factor  $E$ , horizontal shift  $S_H$ , and vertical shift  $S_V$ .

### Slip Calculation

The longitudinal slip velocity  $v_{sx}$  is defined as difference between peripheral speed, i.e. the product of the effective rolling radius  $r_e$  and the relative angular velocity  $\omega_{Rel}$ , and the longitudinal velocity  $v_x$ .

$$V_{sx} = r_e \omega_{Rel} - v_x$$

The lateral slip velocity  $v_{sy}$  equals the lateral velocity  $v_y$ .

$$v_{sy} = v_y$$

The total slip velocity  $v_{st}$  is the absolute value of the slip velocity vector

$$v_s = (v_{sx} \ v_{sy})^T$$

$$v_{st} = \sqrt{(v_{sx}^2 + v_{sy}^2)}$$

The slipping angle  $\alpha_\lambda$  are determined by formulae

$$\cos \cos (\alpha_\lambda) = \frac{v_{sx}}{v_{st}}$$

$$\sin \sin (\alpha_\lambda) = \frac{-v_{sy}}{v_{st}}$$

The longitudinal slip  $\lambda_x$ , the lateral slip  $\lambda_y$  and the total slip  $\lambda_t$  can be obtained by formulae

$$\lambda_x = - \frac{v_{sx}}{r_e \omega_{Rel}}$$

$$\lambda_y = - \frac{v_{sy}}{r_e \omega_{Rel}}$$

$$\lambda_t = - \frac{v_{st}}{r_e \omega_{Rel}}$$

### Tire Forces Calculation

The longitudinal tire force  $F_x$  can be calculated by means of the eight coefficients  $C_x P$  of the magic formula.

The variable  $X_x$  can be interpreted as an equivalent longitudinal slip.

$$X_x = -100 \frac{\lambda_t}{1+\lambda_t}$$

The variable  $B_x$  can be interpreted as stiffness factor of the longitudinal force over slip characteristic curve.

$$B_x = \frac{C_{xP3} F_z^2 + C_{xP4} F_z}{C_x D_x \exp(C_{xP5} F_z)}$$

The shape factor  $C_x$  is set to 1.65 for longitudinal force calculation and can not be changed.

$$C_x = 1.65$$

The variable  $D_x$  can be regarded as peak value of the longitudinal force over slip characteristic curve.

$$D_x = C_{xP1} F_z^2 + C_{xP2} F_z$$

The variable  $E_x$  corresponds to the curvature of the longitudinal force over slip characteristic curve.

$$E_x = C_{xP6} F_z^2 + C_{xP7} F_z + C_{xP8}$$

There is neither a horizontal nor a vertical shift of the longitudinal force over slip characteristic curve, hence the shift parameters  $SH_x$  and  $SV_x$  vanish.

$$\begin{aligned} S_{Hx} &= 0 \\ S_{Vx} &= 0 \end{aligned}$$

Once all parameters are calculated the magic formula can be applied to finally get the longitudinal tire force.

$$\begin{aligned} Y_x &= D_x \sin \sin \left( C_x \arctan \arctan \left( B_x (1 - E_x) (X_x + S_{Hx}) + E_x \arctan \arctan \left( B_x (X_x + S_{Hx}) \right) \right) \right) + S_{Vx} \\ F_x &= Y_x \cos \cos (\alpha_\lambda) \end{aligned}$$

The lateral tire force  $F_y$  is calculated in a similar fashion as  $F_x$  as follows

$$B_y = \frac{C_{yP3} \sin \sin \left( C_{yP4} \arctan \arctan \left( C_{yP5} F_z \right) \right)}{C_y D_y} \left( 1 - C_{yP12} \gamma \right)$$

$$C_y = 1.3$$

$$D_y = C_{yP1} F_z^2 + C_{yP2} F_z$$

$$E_y = \frac{C_{yP6} F_z^2 + C_{yP7} F_z + C_{yP8}}{1 - C_{yP13} \gamma}$$

$$S_{Hy} = C_{yP9} \gamma$$

$$S_{Vy} = \left( C_{yP10} F_z^2 + C_{yP11} F_z \right) \gamma$$

$$\begin{aligned} Y_y &= D_y \sin \sin \left( C_y \arctan \arctan \left( B_y (1 - E_y) (X_y + S_{Hy}) + E_y \arctan \arctan \left( B_y (X_y + S_{Hy}) \right) \right) \right) + S_{Vy} \\ F_y &= Y_y \sin \sin (\alpha_\lambda) \end{aligned}$$

## Self-Aligning Torque

The self-aligning torque  $T_z$  is similarly calculated similar to the lateral and longitudinal forces. The computation of coefficients  $X_n, B_n, C_n, D_n, E_n, S_{Hn}, S_{Vn}$  is done in a similar way. Then  $Y_n$  and  $T_z$  are calculated as follows

$$Y_n = D_n \sin \sin (C_n \arctan \arctan (B_n (1 - E_n) (X_n + S_{Hn}) + E_n \arctan \arctan (B_n (X_n + S_{Hn}))) ) + S_{Vn}$$

$$T_z = -Y_n \sin \sin (\alpha_\lambda)$$

## Tire Dynamics

A linear three-dimensional spring and damper system with stiffness  $k = (k_x, k_y, k_z)^T$  and damping coefficient  $b = (b_x, b_y, b_z)^T$  is introduced to incorporate the first order tire dynamics. The vertical force  $F_z$  is then calculated by the following spring-damper equation along the Z-direction of the wheel axis coordinate system

$$F_z = k_z d_{xz} + b_z d_{vz}$$

where  $dx$  is the three-dimensional vector of tire deformation and  $dv$  is the vector of deformation velocity

## Effective Rolling Radius

The calculation of effective rolling radius  $r_e$  follows a magic formula approach

$$r_e = r - \frac{F_{zN}}{k_z} (C_{r2} \arctan \arctan \left( \frac{C_{r1} d_{xz} k_z}{F_{zN}} \right) + \frac{C_{r3} d_{xz} k_z}{F_{zN}})$$

Figure shows the dependency of the effective rolling radius  $r_e$  on the vertical deformation  $d_{xz}$

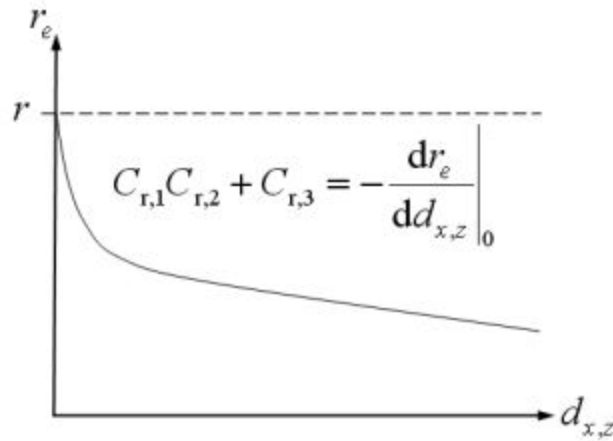


Figure 8: Effective rolling radius characteristic curve

The three coefficients of the radius characteristics  $Cr$  can be interpreted as low load stiffness, peak value and high load stiffness of the effective rolling radius.

### **Overturning Torque**

The overturning torque  $T_x$  is approximated according to reference by formula

$$T_x = -\frac{1}{12} w^2 k_z \gamma$$

where  $w$  is the width of the unloaded tire.

### **Rolling Resistance Torque**

The rolling resistance torque  $T_y$  is calculated as follows

$$T_y = -\mu_r r F_z \{ \text{sign}(v_x) \quad \text{if } |v_x| > v_e \frac{v_x}{v_e} \quad \text{if } |v_x| \leq v_e$$

Where  $v_e$  is a small threshold longitudinal velocity to make sure the torque curve is continuous and  $\mu_r$  is the rolling resistance coefficient.

### **Parameterization**

The following parameters are input into the corresponding elements

Rolling Resistance  $\mu_r = 0.005$  [5]

#### **Tire elastic properties** [6][7]

Tire Vertical Stiffness  $k[3] = 500$  kN/m

Tire Vertical Damping  $b[3] = 261$  Ns/m

#### **Tire Geometry** [8]

Wheel Radius  $rW = 21.95$  in

Tire Width  $wT = 11$  in

## Masses

The masses of the elements present in the tire assembly are captured through the *tireMassDrive*, *rimMassDrive*, *brakeDiscMassDrive* elements whose values are 125.7 lbs, 51 lbs, 22 lbs respectively [8][9].

In addition, an imbalance mass of 8 oz for the tire and a miscellaneous imbalance (from drive shaft, brake disc wear etc.) of 2 oz are captured at the circumference of each tire.

In the presence of a balancer all the imbalance mass and an additional 11 lbs (*Centramatic* balancer for drive and trailer axles) is captured at the center of the wheel.

### 2.1.4 Work Done Computation

The *presetDrive* element in figure 3 is used to set an rpm as a boundary condition to the tire model. This element gives out the power required to run the truck at that particular speed. This power is read into the *powerDrive* element in figure 4 which is then integrated in the *workDrive* element to compute the total work done. This work done is then multiplied by 4 inside the *workAllDriveWheels* to capture the work done by all the drive wheels. The same computation is extended to the trailer and steer axles to compute the total work done by the truck. The total work done is then computed with and without the balancers and the resulting energy savings are computed as follows

$W_o$  = Work done without the balancers

$W_n$  = Work done with the balancers

$$\text{Energy Savings (\%)} = \frac{(W_o - W_n) * 100}{W_o}$$

## 2.2 Steer Axle Setup

The steer axle has a similar setup to the drive/trailer axle as seen in figure but with the following changes

- An additional air drag resistance on the truck captured as follows
  - o Drag Force  $F_d = 0.5 * C_d * \rho * A * v^2$   
Where  $C_d$  is the drag coefficient (a value of 0.51 assumed),  $A$  is the frontal area (75.3 sq ft i.e. 7 m<sup>2</sup>) assumed,  $\rho$  is the air density,  $v$  is the relative truck speed.
  - o Total drag force is then divided by 2 to account for the full steer axle
- Effective axle load in the *wheelLoadSteer* element set to 12,000/2 lbs

- The damping coefficient in the *damper3* element is set to 0.7 times the damping coefficient of the damper in the drive/trailer axle to account for lesser load per one side of the axle (34000/4 lbs vs 12,000/2 lbs)
- Tire and rim geometry, masses based on [9] [10]
- Balancer mass of 6 lbs (*Centramatic* balancer for steer axles)
- Total work done multiplied by 2 for 2 steer wheels

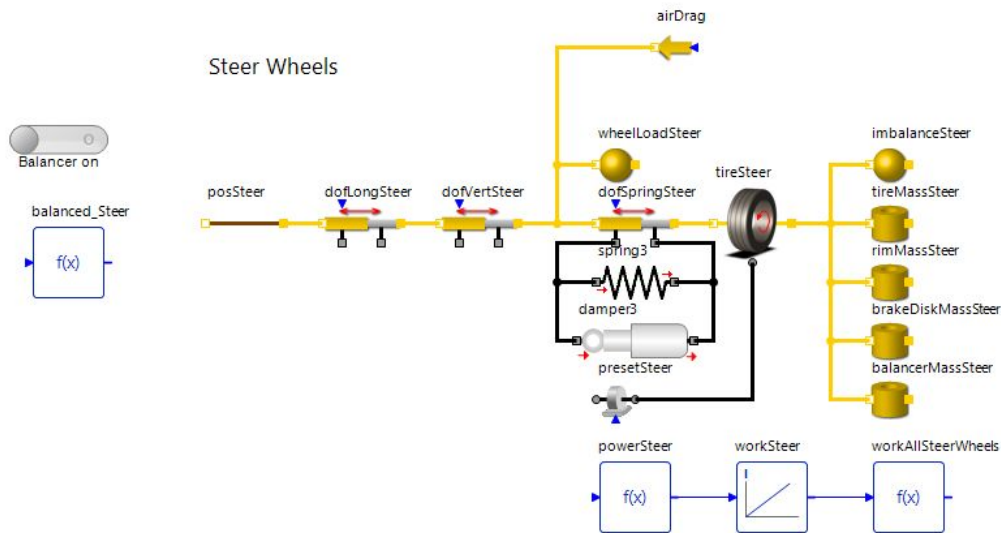


Figure 9: Steer axle setup

### 3. Scenario Setup and Results

The test scenario is setup in the following way

- Truck runs at a constant speed of 57.5 mph for 2 hours
- A damping degradation of 30% assumed
- The work done at all the drive, trailer and steer wheels is added and total work done is computed in both the scenarios

Figures 10 and 11 show the velocity difference ( $dv$ ) profile across the shock absorber without and with the balancer respectively with an imbalance of 8 oz. As seen from the figures, the presence of balancer suppresses all the oscillations resulting in energy savings. The energy savings, which is computed based on the section 2.1.4 is shown in the table 1

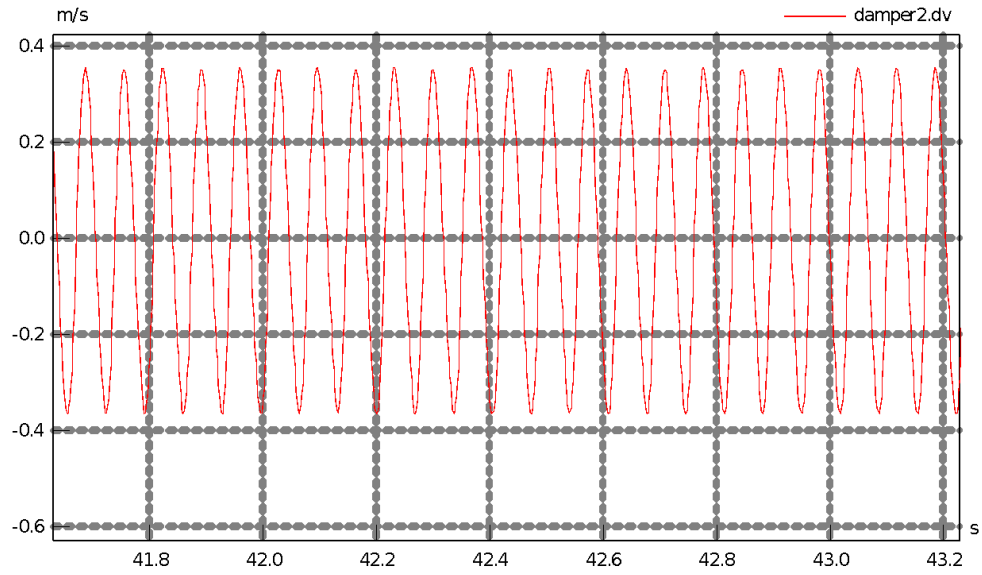


Figure 10: Velocity difference across the shock absorber – no balancer

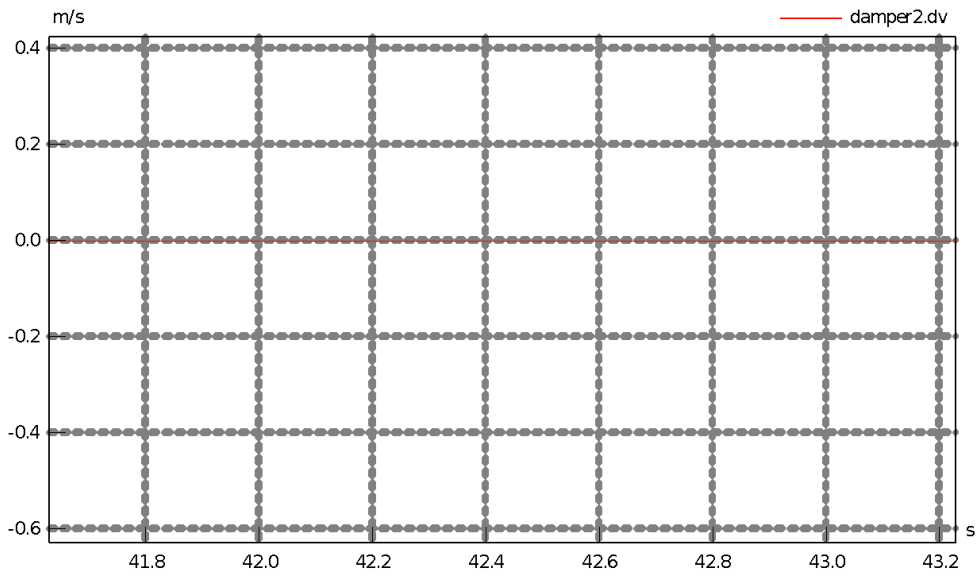


Figure 11: Velocity difference across the shock absorber – with balancer

<b>Energy Savings</b>		
Average imbalance per tire (oz)	8	<b>2.11%</b>
Miscellaneous imbalance per tire (oz)	2	
Work done without balancers $W_o$ (kWh)	<b>170.833</b>	
Work done with balancers $W_n$ (kWh)	<b>167.222</b>	

Table 1: Energy savings calculation

#### 4. Summary

A network-based simulation approach was followed to determine the fuel savings in the presence of *Centramatic* wheel balancers. As seen from the results, *Centramatic* wheel balancers offers fuel savings of about 2.11%. These fuel savings can be completely attributed to the presence of wheel balancers as the model gives the flexibility of maintaining exact same physical conditions when performing tests with and without the wheel balancers. In addition, the balancers also offer much quieter ride as seen from the vibration reduction. This would also lead to much longer tire life i.e. less tread wear thereby resulting in an even increased cost savings.

#### 5. References

- [1] [https://www.eia.gov/energyexplained/index.php?page=us\\_energy\\_transportation#tab2](https://www.eia.gov/energyexplained/index.php?page=us_energy_transportation#tab2)
- [2] Yongjie Lu, Shaohua Li and Na Chen, Research on Damping Characteristics of Shock Absorber for Heavy Vehicle, Institute of Mechanical Engineering, Shijiazhuang Tiedao University, Shijiazhuang, China
- [3] J.J.M. van Oosten, H.-J. Unrau, A. Riedel, and E. Bakker: Standardization in Tire Modeling and Tire Testing - TYDEX Workgroup, TIME Project, Tire Science and Technology, Volume 27, Issue 3, pp. 188-202, July 1999.
- [4] E. Bakker, L. Nyborg, and H.B. Pacejka: Tire Modelling for Use in Vehicle Dynamics Studies. Society of Automotive Engineers, January 1987.
- [5] Germana Paterlini, Rolling Resistance Validation, Minnesota Department of Transportation, Principal Investigator, FuelMiner, Inc.
- [6] [https://tigerprints.clemson.edu/cgi/viewcontent.cgi?article=1123&context=all\\_theses](https://tigerprints.clemson.edu/cgi/viewcontent.cgi?article=1123&context=all_theses)

- [7] [https://ir.library.dc-uoit.ca/bitstream/10155/523/1/Reid\\_Adam\\_C.pdf](https://ir.library.dc-uoit.ca/bitstream/10155/523/1/Reid_Adam_C.pdf)
- [8] <https://www.otrusa.com/product/11r24-5-h-bf-goodrich-dr444-drive/>
- [9] [https://www.arconic.com/alcoawheels/north-america/en/products/product.asp?prod\\_id=4591](https://www.arconic.com/alcoawheels/north-america/en/products/product.asp?prod_id=4591)
- [10] <https://www.otrusa.com/product/11r24-5-h-bf-goodrich-st244-steer/>
- [11] [www.simulationx.com](http://www.simulationx.com)